Published in final edited form as:
Hepatology. 2014 December ; 60(6): 2065–2076. doi:10.1002/hep.27348.

Mouse Hepatocyte Overexpression of NF-κB-inducing Kinase (NIK) Triggers Fatal Macrophage-dependent Liver Injury and Fibrosis

Hong Shen, **Liang Sheng**, **Zheng Chen**, **Lin Jiang**, **Haoran Su**, **Lei Yin**, **M. Bishr Omary**, and **Liangyou Rui***
Department of Molecular & Integrative Physiology, University of Michigan Medical School, Ann Arbor, MI 48109, USA

Abstract

Damaged, necrotic, or apoptotic hepatocytes release damage-associated molecular patterns that initiate sterile inflammation, and liver inflammation drives liver injury and fibrosis. Here we identified hepatic NF-κB-inducing kinase (NIK), a Ser/Thr kinase, as a novel trigger of fatal liver inflammation. NIK is activated by a broad spectrum of stimuli. It was upregulated in injured livers in both mice and humans. In primary mouse hepatocytes, NIK overexpression stimulated, independently of cell injury and death, release of numerous chemokines and cytokines that activated bone marrow-derived macrophages (BMDMs). BMDMs in turn secreted pro-apoptotic molecules that stimulated hepatocyte apoptosis. Hepatocyte-specific expression of the *NIK* transgene triggered massive liver inflammation, oxidative stress, hepatocyte apoptosis, and liver fibrosis, leading to weight loss, hypoglycemia, and death. Depletion of Kupffer cells/macrophages reversed NIK-induced liver destruction and death.

Conclusion—the hepatocyte NIK-liver immune cell axis promotes liver inflammation, injury and fibrosis, thus driving liver disease progression.

Keywords

liver inflammation; hepatocyte apoptosis; Kupffer cells

INTRODUCTION

The liver regulates many vital physiological processes, and liver inflammation plays a critical pathological role in liver disease progression (1-4). Injured, necrotic, and apoptotic hepatocytes release damage-associated molecular patterns (DAMPs) which are believed to initiate liver inflammation (2-4). Hepatocytes also express cytokines and chemokines (5-7); however, their contributions to liver disease are not fully understood.

We recently reported that nonalcoholic fatty liver disease (NAFLD) is associated with abnormal activation of NF-κB-inducing kinase (NIK, also called MAP3K14) in the liver (8).

*To whom correspondence should be addressed: Liangyou Rui, Ph.D. Department of Molecular & Integrative Physiology University of Michigan Medical School Ann Arbor, MI 48109, USA Tel.: (734) 615-7544; Fax: 734-647-9523; ruily@umich.edu.

NIK is a ubiquitously-expressed Ser/Thr kinase, and its levels are very low due to rapid proteasome-mediated degradation (9, 10). In quiescent cells, the TRAF2/TRAF3 adaptor protein complex binds to NIK and recruits NIK to cIAP1/2 ubiquitin E3 ligases, resulting in NIK ubiquitination and degradation (10-12). NIK is activated by diverse stimuli, including oxidative stress, saturated fatty acids, cytokines, endotoxins, as well as ligands that activate TLRs, receptor tyrosine kinases, and G protein-coupled receptors (8, 13-18). Cytokines stimulate TRAF3 degradation, leading to NIK stabilization and activation (19, 20). NIK is required for the activation of the noncanonical NF-κB2 signaling pathway (21). It phosphorylates and activates IKKα which in turn phosphorylates the p100 form of NF-κB2 (22, 23). Phosphorylation of p100 promotes its proteolytic cleavage to generate the mature p52 form of NF-κB2 (13, 21, 23).

NIK is known to regulate lymphocyte development and adaptive immunity (13, 14). We asked whether NIK in hepatocytes is involved in regulating liver inflammation, integrity, and function. We have generated and characterized new mouse models with hepatocyte-specific overexpression of the *NIK* transgene, and have examined NIK-induced crosstalk between hepatocytes and immune cells. Our data demonstrate that hepatic NIK is a previously-unknown regulator of liver inflammation and liver integrality.

EXPERIMENTAL PROCEDURES

Animals

Mice were housed on a 12-h light-dark cycle in the Unit for Laboratory Animal Medicine at the University of Michigan. Animal experiments were conducted following the protocols approved by the University Committee on the Use and Care of Animals.

STOP-Tomato reporter mice and *albumin-Cre* transgenic mice (C57BL/6 background) were from the Jackson Laboratory (Bar Harbor, ME). *STOP-NIK* mice (C57BL/6 background) were kindly provided by Dr. Klaus Rajewsky (Harvard Medical School, Boston, MA) (24). Adult *STOP-NIK* mice were infected with *albumin*-Cre adenoviruses or AAV-Cre via tail vein injection to activate the *NIK* transgene specifically in hepatocytes. Alternatively, *STOP-NIK* mice were crossed with *albumin-Cre* transgenic mice to specifically activate the *NIK* transgene in hepatocytes of *STOP-NIK* and *albumin-Cre* double transgenic mice. Kupffer cells/macrophages were depleted by $GdCl_3$ treatments as reported previously (25, 26).

Immunostaining, immunoblotting and qPCR

Liver paraffin or frozen sections were prepared and immunostained with the indicated antibodies. Liver extracts were blotted with the indicated antibodies. Liver mRNA abundance was quantified by qPCR.

Primary hepatocyte cultured and cell death assays

Primary hepatocytes were prepared from mice, and were either grown alone or cocultured with BMDMs. Cell death was measured by Terminal deoxynucleotidyl transferase dUTP nick end labeling (TUNEL) assays.

Detailed methods were described in the Supplemental Materials.

Statistics

Data were presented as means ± s.e.m. Differences between groups were analyzed with two-tailed Student's t test. $P < 0.05$ was considered statistically significant.

RESULTS

NIK is aberrantly activated in damaged livers in mice and humans

Liver injury was induced by treating mice with CCl_4 or alcohol. Both CCl_4 and 3-week alcohol treatments significantly increased *NIK* mRNA levels (Fig. 1A-B). Hepatic NIK protein was undetectable by commercial antibodies (8, 10), so we estimated NIK activation by examining the noncanonical NF-κB2 pathway. Both CCl_4 treatments and chronic alcohol consumption markedly increased the amounts of the p52 form of NF-κB2 (Fig. 1D-E). We asked whether hepatic NIK is overactivated in human liver disease. Liver biopsies were obtained from normal subjects and patients with alcoholic cirrhosis or primary biliary cirrhosis (PBC). The levels of both *NIK* mRNA (Fig. 1C) and p52 protein (Fig. 1F) were higher in cirrhotic livers.

Adult-onset, hepatocyte-specific activation of NIK causes liver dysfunction and death in mice

To examine the role of NIK, we obtained *STOP-NIK* mice in which a "*STOP-NIK*" transgenic cassette was inserted into the *Rosa26* locus (24). Cre-mediated incision of the "*STOP*" sequences, which are flanked by a loxp site at both ends, is expected to activate the *NIK* transgene whose expression is under the control of the endogenous *Rosa26* promoter (8, 24). We generated *albumin*-Cre adenoviruses in which *Cre* expression is under the control of the mouse *albumin* promoter. To validate the adenoviruses, *STOP-Tomato* reporter mice, which had a similar *STOP-Tomato* knock-in cassette at the *Rosa26* locus, were infected with *albumin*-Cre adenoviruses via tail vein injection. Liver sections were immunostained with antibodies against keratin-18 (a liver epithelial cell marker), keratin-19 (a cholangiocyte marker), or F4/80 (a Kupffer cell/macrophage marker). Tomato-red fluorescence was detected only in hepatocytes but not in cholangiocytes, Kupffer cells, and macrophages (Fig. S1A). Tomato-red fluorescence was also detected in purified primary hepatocytes (albumin- and K18-positive cells) (Figs. S1B-C).

STOP-NIK mice (8-9 weeks) were infected with *albumin*-Cre or green fluorescent protein (GFP) adenoviruses via tail vein injection. Recombinant NIK (with a N-terminal Flag tag) and high levels of p52 were detected in the livers of Cre, but not GFP, adenovirus-infected mice (Fig. 2A-B). Recombinant NIK was absent in the heart, adipose tissue, kidney, and skeletal muscle (Fig. 2A). Mice with hepatocyte-specific overexpression of NIK progressively lost their body weights, developed hypoglycemia, and died gradually with 90% lethality 27 days after infection (Fig. 2C). In contrast, none of GFP adenovirus-infected mice died 27 days after infection, which was the extent of time the animals were followed. The activity of serum alkaline phosphatase (ALP) and alanine aminotransferase (ALT) and the levels of total bilirubin were significantly higher in Cre than in GFP groups (Fig. 2D). As a control, *albumin*-Cre-infected wild type (WT) mice did not have weight loss, hypoglycemia, and liver injury (Figure S2A-B). To verify these observations, we infected

STOP-NIK mice with AAV-Cre. NIK was specifically overexpressed in the liver (Fig. S3A), and caused weight loss, hypoglycemia and fatal liver injury (Fig. 2E-F). These findings indicate that hepatocyte-specific overexpression of NIK is sufficient to cause lethal liver injury.

Adult-onset overexpression of NIK in hepatocytes promotes liver oxidative stress and hepatocyte apoptosis in mice

Hepatocyte-specific overexpression of NIK caused hepatomegaly in *STOP-NIK* mice infected with either *albumin*-Cre (Fig. 3A) or AAV-Cre (Fig. S3B). Liver architectures were disrupted, with many damaged ballooned hepatocytes and massive immune cell infiltration (Fig. 3B and Fig. S3C). The number of apoptotic liver cells, measured by TUNEL assays, was significantly higher in NIK-overexpressing mice (Fig. 3C-D). The amount of active caspase-3 (casp3), apoptotic keratin-18 fragment, and phosphorylated JNKs were also higher (Fig. 3E). Apoptotic keratin-18 fragments have been used to estimate hepatocyte death (27). The levels of reactive oxygen species (ROS) were significantly higher in both *albumin*-Cre and AAV-Cre groups (Fig. 3F). By contrast, *albumin*-Cre infection did not cause hepatomegaly, liver oxidative stress, inflammation, and hepatocyte apoptosis in WT mice (Fig. S2B-E). These observations suggest that hepatocyte-specific overexpression of NIK promotes liver oxidative stress and hepatocyte apoptosis, leading to fatal liver injury.

Adult-onset, hepatocyte-specific overexpression of NIK causes liver inflammation and fibrosis

To examine liver inflammation, liver sections were immunostained with antibodies to F4/80, CD45, or CD3. Kupffer cell/macrophage number was significantly higher in *albumin*-Cre (Fig. 4A) and AAV-Cre groups (Fig. S3D-E). The numbers of CD45-positive and CD3-positive cells were also higher in the *albumin*-Cre group (Fig. S4). The expression of liver chemokines (e.g. CCL2, CCL5 and CXCL5), proinflammatory cytokines (e.g. TNFα and IL-6), and inducible nitric oxide synthase (iNOS) was much higher in *albumin*-Cre than in GFP adenovirus-infected mice (Fig. 4B). To examine liver fibrosis, liver sections were stained with Sirius-red. Liver fibrillar collagen was barely detectible in the GFP group, but very abundant in both *albumin*-Cre (Fig. 4C) and AAV-Cre groups (Fig. S3C). Liver hydroxyproline content, an index to estimate liver fibrosis, was significantly higher in both *albumin*-Cre (Fig. 4D) and AAV-Cre groups (Fig. S3B). We measured liver α-smooth muscle actin (α-SMA), a marker for activated myofibroblasts, by immunoblotting and immunostaining. α-SMA was barely detectable in the GFP group, but readily observed in both *albumin*-Cre (Fig. 4E-F) and AAV-Cre groups (Fig. S3F). The expression of profibrotic genes (e.g. *TGFβ1*, *αSMA*, *vimentin*, *collagen 1a1*, and *TIMP*) in the liver were significantly increased by hepatocyte-specific overexpression of NIK (Fig. 4B). In contrast, *albumin*-Cre infection did not cause liver fibrosis in WT mice (Fig. S2B-C). These data indicate that hepatocyte-specific overexpression of NIK is sufficient to promote liver inflammation, myofibroblast activation, and liver fibrosis.

Embryonic onset, hepatocyte-specific expression of NIK causes liver injury, inflammation, and fibrosis

To further verify NIK action, we generated *NIK* transgenic (Tg) mice by crossing *STOP-NIK* mice with *albumin-Cre* mice. Both heterozygous ($Tg^{+/-}$, genotype: *STOP-NIK*$^{+/-}$;*Cre*$^{+/-}$) and homozygous ($Tg^{+/+}$, genotype: *STOP-NIK*$^{+/+}$;*Cre*$^{+/-}$) transgenic mice were generated, and *STOP-NIK* mice (genotype: *STOP-NIK*$^{+/+}$;*Cre*$^{-/-}$) were used as control (Con). The *NIK* transgene was expressed in the livers of $Tg^{+/-}$ and $Tg^{+/+}$ but not Con mice, and *NIK* mRNA levels were much higher in $Tg^{+/+}$ than in $Tg^{+/-}$ mice (Fig. S5A). The p52 form of NF-κB2 in the liver was detected only in $Tg^{+/+}$, but not in $Tg^{+/-}$ and Con, mice (Fig. S5B), suggesting that a threshold level of NIK is required for the activation of its downstream pathways.

$Tg^{+/+}$ mice gained significantly less body weight than $Tg^{+/-}$ and Con mice (Fig. 5A). $Tg^{+/-}$ mice were grossly normal. Like *STOP-NIK* mice infected with *albumin*-Cre- or AAV-Cre, $Tg^{+/+}$ mice became severely ill and were euthanized after 12 weeks of age. Serum ALT activity and bilirubin levels were significantly higher in $Tg^{+/+}$ than in $Tg^{+/-}$ and Con mice (Fig. 5B). Liver function was impaired in $Tg^{+/+}$ mice as revealed by hypoglycemia (Fig. 5A). Liver weight and ROS levels were significantly higher in $Tg^{+/+}$ than in Con mice (Fig. 5C). $Tg^{+/+}$ livers had dying hepatocytes and massive immune cell infiltration (Fig. 5D). Liver apoptosis was 23-fold higher in $Tg^{+/+}$ than in Con mice (Fig. 5E). Caspase-3 and JNK activation was also higher in $Tg^{+/+}$ mice (Fig. 5F).

$Tg^{+/+}$ mice developed severe liver inflammation (Fig. 6A-B and Fig. S5C-D) and fibrosis (Fig. 6C-F). Unlike $Tg^{+/+}$ mice, $Tg^{+/-}$ mice had neither liver injury nor liver fibrosis (Fig. 6). Therefore, a threshold level of hepatic NIK is required to activate lethal liver inflammation, injury, and fibrosis.

Inflammation mediates NIK-induced liver injury, liver fibrosis, and death

We depleted Kupffer cells/macrophages by $GdCl_3$ treatments as reported previously (25, 26). In the H_2O-treated group (control), hepatocyte-specific overexpression of NIK caused progressive weight loss, hypoglycemia and death, and $GdCl_3$ treatment largely protected against these detrimental effects of NIK (Fig. 7A-B). Depletion of Kupffer cells/macrophages also prevented NIK-induced liver injury (Fig. 7C). $GdCl_3$ treatment markedly decreased immune cell infiltration and Kupffer cell/macrophage number in the liver (Fig. 7D and Fig. S6A-B). Depletion of Kupffer cells/macrophages dramatically decreased NIK-induced liver oxidative stress, apoptosis, myofibroblast activation, and fibrosis (Fig. 7D and Fig. S6B-E), and attenuated NIK-induced activation of hepatic caspase-3 and JNKs (Fig. 7E). Hepatocyte-specific overexpression of NIK increased the expression of proapoptotic genes (e.g. *Bim, Noxa, FAS,* and *DR5*) in the liver, which was reversed by $GdCl_3$ treatments (Fig. 7F). Together, these data indicate that hepatocyte-specific overactivation of NIK triggers lethal inflammation.

Hepatic NIK stimulates innate immunity independently of hepatocyte injury and death

To examine cell-autonomous action of hepatic NIK, we measured hepatocyte survival (MTT assays) and apoptosis (TUNEL assays). NIK was overexpressed in primary hepatocytes via

NIK adenoviral infection, and β-galactosidase (β-Gal) adenovirus was used as control (Fig. 8A). NIK neither decreased survival nor increased apoptosis; in contrast, survival rates were higher in NIK-overexpressing hepatocytes 4 days after infection (Fig. 8B). ROS levels and ALT release were also similar between control and NIK-overexpressing hepatocytes (Fig. S7A, S7C left half). Thus, NIK activation alone is unable to directly induce hepatocyte injury and death.

NIK markedly increased the expression of CCL2, CCL5, CXCL5, and TNFα in primary hepatocytes (Fig. 8C upper panels). We prepared conditioned media from primary hepatocytes infected with either β-Gal or NIK adenoviruses, and measured their ability to activate bone marrow-derived macrophages (BMDMs). NIK-conditioned medium stimulated 4-1600-fold higher expression of CCL2, CCL5, CXCL5, TNFα, IL-6 and iNOS in BMDMs, compared with β-Gal-conditioned medium; in contrast, the expression of IL-10, an immunosuppressive cytokine, was 85% lower in BMDMs treated with NIK-conditioned medium (Fig. 8C lower panels). Heating treatments markedly decreased the ability of NIK-conditioned medium to activate BMDMs (Fig. S7B). These data indicate that hepatocyte NIK pathways potently stimulate the production and release of heat-labile proinflammatory mediators which in turn activate innate immune cells.

Aberrant activation of hepatic NIK triggers a hepatocyte suicide program through activating innate immune cells

Primary hepatocytes were infected with NIK or β-Gal adenoviruses and subsequently co-cultured without (Con) or with BMDMs, and apoptosis was measured by TUNEL assays. In the absence of BMDMs, overexpression of NIK did not cause apoptosis; in contrast, NIK overexpression caused massive hepatocyte apoptosis in the presence of BMDMs (Fig. 8D). Overexpression of NIK in hepatocytes also caused hepatocyte injury, as estimated by ALT release, in the presence, but not in the absence, of BMDMs (Fig. S7C). To verify these results, primary hepatocytes were isolated from *STOP-NIK* mice and infected with GFP (control) or *albumin*-Cre adenoviruses. Cre-mediated activation of the *NIK* transgene also increased the expression of multiple proinflammatory cytokines (Fig. S7D), and induced hepatocyte apoptosis in a BMDM-dependent fashion (Fig. 8E and Fig. S7E).

To gain insight into potential downstream pathways, we generated $NIK^{K429,430A}$ (called KA) and G885R, NIK mutants which lack catalytic activity or ability to activate the noncanonical NF-κB2 pathway, respectively (8, 22, 28). Primary hepatocytes were infected with β-Gal, NIK, G885R or KA adenoviruses, and the levels of NIK, G885R and KA were comparable (Fig. S8A). NIK, but not G885R and KA, robustly activated the noncanonical NF-κB2 pathway (Fig. S8B-D). Like NIK, G885R stimulated massive hepatocyte apoptosis in a BMDM-dependent manner (Fig. 8D and Fig. S8E). Both NIK and G885R activated caspase-3 in hepatocytes in a BMDM-dependent manner (Fig. 8F). G885R-conditioned medium also potently stimulated the expression of CCL2, CCL5, CXCL5, IL-1, IL-6, TNFα and iNOS in DMBMs (Fig. S8F). In contrast, overexpression of KA did not cause hepatocyte apoptosis, caspase-3 activation, and release of proinflammatory mediators from hepatocytes (Figs. 8D and 8F, and Fig. S8E-F). Therefore, NIK catalytic activity, but not its

ability to activate the noncanonical NF-κB2 pathway, is required for the NIK action in hepatocytes.

To examine the role of the canonical NF-κB1 pathway, we prepared conditioned medium from hepatocytes overexpressing constitutively-active IKKβ(SE) variant. IKKβ(SE)-conditioned medium was unable to stimulate the expression of CCL5 and iNOS, and was 28-592-fold less potent, compared with NIK-conditioned medium, to stimulate the expression of CCL2, CXCL5, IL-1, and IL-6 (Fig. S8F).

DISCUSSION

In this study, we have established a new concept that hepatocyte NIK pathways trigger fatal liver inflammation independently of hepatocyte injury and death, leading to liver fibrosis and destruction.

Hepatic NIK triggers lethal liver inflammation

NIK-overexpressing primary hepatocytes are not damaged, apoptotic, or necrotic, so hepatic NIK is less likely to cause inflammation through DAMP release. Conditioned medium from NIK-overexpressing hepatocytes, which was sensitive to heating, robustly stimulated BMDMs to express CCL2, CCL5, CXCL5, TNFα, IL-6 and iNOS, indicating that NIK promotes hepatocytes to release heat-sensitive mediators that activate immune cells. In agreement, hepatic NIK cell-autonomously stimulated the expression of many chemokines and cytokines, including CCL2, CCL5, CXCL5, and TNFα. The canonical and noncanonical NF-κB pathways are less likely to mediate NIK action, because G885R, which is unable to activate the noncanonical NF-κB2 pathway (22, 28), acted as NIK to stimulate hepatocyte release of proinflammatory mediators, whereas IKKβ(SE), which activates the canonical NF-κB1 pathway, was unable to do so. Unlike *NIK* transgenic mice, hepatocyte-specific *IKKβ* transgenic mice are viable and have normal body weight and very mild liver injury (29). Aside from IKKα and IKKβ, NIK also phosphorylates other substrates, including CREB and p38 (8, 30). Thus, NIK is likely to control a complex program which coordinates the expression and secretion of proinflammatory mediators. The pattern and network of these mediators, rather than individual mediators, are likely to trigger liver inflammation.

NIK-induced liver inflammation may develop through several stages. Initially, NIK-stimulated, hepatocyte-derived mediators trigger immune cell recruitments and activation. In the second stage, immune cell-derived mediators further recruit and activate additional immune cells, thus forming a recruitment→chemokine/cytokine release→additional recruitment vicious cycle. Additionally, Hepatocyte- and immune cell-derived mediators may activate hepatic stellate cells (HSCs), which in turn promote inflammation by secreting additional proinflammatory mediators.

NIK-induced inflammation triggers live injury and fibrosis

NIK overexpression in hepatocytes alone was insufficient to cause apoptosis, and NIK-expressing hepatocytes died only in the presence of BMDMs. Moreover, depletion of Kupffer cells/macrophages largely eliminated NIK-induced liver oxidative stress and

hepatocyte death, and reversed liver failure and death. These results indicate that hepatocyte NIK signaling instructs innate immune cells via hepatocyte-derived mediators, and the "educated" immune cells subsequently execute hepatocyte death via releasing hepatotoxic factors. Moreover, NIK overexpression markedly increased the expression of plasma membrane death receptors (e.g. FAS and DR5) and intracellular pro-apoptotic molecules (e.g. Bim and Noxa) in the liver, suggesting that NIK signaling may also increase hepatocyte sensitivity to death signals.

Hepatocyte-specific overexpression of NIK also activated HSCs and myofibroblasts, leading to liver fibrosis. HSC/myofibroblast activation is likely to be secondary to NIK-induced liver inflammation. However, NIK-stimulated, hepatocyte-derived mediators may also directly activate HSCs, contributing to liver inflammation and fibrosis.

Hepatic NIK promotes liver disease progression

The expression and activity of hepatic NIK were higher in both rodents and humans with liver disease. NIK may be activated by a broad spectrum of stimuli present during liver disease progression. A modest increase in hepatic NIK was unable to activate liver NF-κB2 and JNK pathways and liver inflammation and fibrosis in $Tg^{+/-}$ mice. A further increase caused activation of the NF-κB2 and JNK pathways and lethal liver inflammation, fibrosis, and destruction in homozygous $Tg^{+/+}$ mice. Therefore, a threshold level of hepatic NIK is required to fully activate the liver destruction program.

NIK expression is very low, most-likely below the NIK threshold, in normal livers (8, 10). Genetic and/or environmental risk factors (e.g. alcohol, drugs and other toxins, hepatic steatosis, oxidative stress, and inflammation) may increase hepatocyte NIK levels and activity above the threshold, leading to activation of the NIK destruction program. Indeed, the levels of p52 NF-κB2 in the liver were higher in both mice and humans with liver injury. Alternatively, these factors may lower the NIK threshold, thus activating the NIK destruction program. Finally, the genetic and environmental insults may functionally interact with the sub-threshold levels of hepatic NIK in an additive or synergistic fashion to promote liver disease progression.

In conclusion, we have identified hepatic NIK as a novel trigger of the liver inflammation and destruction program under pathological conditions. Hepatic NIK may serve as a therapeutic target in treating liver injury and liver disease.

Supplementary Material

Refer to Web version on PubMed Central for supplementary material.

Acknowledgments

We thank Drs. Natasha Snider, Vithanage Sujith Weerasinghe, Yatrik Shah, and Ms Suqing Wang for assistance and discussion. We thank Dr. Klaus Rajewsky (Immune Disease Institute, Harvard Medical School, Boston, MA 02115) for providing *STOP-NIK* mice.

Financial Support: This study was supported by grants DK091591 and DK094014 from the National Institutes of Health. This work utilized the cores supported by the Michigan Diabetes Research and Training Center (NIH

DK20572), the University of Michigan's Cancer Center (NIH CA46592), the University of Michigan Nathan Shock Center (NIH P30AG013283), and the University of Michigan Gut Peptide Research Center (NIH DK34933).

Abbreviations

NIK	NF-κB-inducing kinase
BMDMs	bone marrow-derived macrophages
GFP	green fluorescent protein
α-SMA	α-smooth muscle actin
ROS	reactive oxygen species
ECM	extracellular matrix

References

1. Rui L. Energy metabolism in the liver. Compr Physiol. 2014; 4:177–197. [PubMed: 24692138]
2. Imaeda AB, Watanabe A, Sohail MA, Mahmood S, Mohamadnejad M, Sutterwala FS, Flavell RA, et al. Acetaminophen-induced hepatotoxicity in mice is dependent on Tlr9 and the Nalp3 inflammasome. J Clin Invest. 2009; 119:305–314. [PubMed: 19164858]
3. McGill MR, Sharpe MR, Williams CD, Taha M, Curry SC, Jaeschke H. The mechanism underlying acetaminophen-induced hepatotoxicity in humans and mice involves mitochondrial damage and nuclear DNA fragmentation. J Clin Invest. 2012; 122:1574–1583. [PubMed: 22378043]
4. Tsung A, Sahai R, Tanaka H, Nakao A, Fink MP, Lotze MT, Yang H, et al. The nuclear factor HMGB1 mediates hepatic injury after murine liver ischemia-reperfusion. J Exp Med. 2005; 201:1135–1143. [PubMed: 15795240]
5. Sheng L, Jiang B, Rui L. Intracellular lipid content is a key intrinsic determinant for hepatocyte viability and metabolic and inflammatory states in mice. Am J Physiol Endocrinol Metab. 2013; 305:E1115–1123. [PubMed: 23982157]
6. Dibra D, Cutrera J, Xia X, Kallakury B, Mishra L, Li S. Interleukin-30: a novel antiinflammatory cytokine candidate for prevention and treatment of inflammatory cytokine-induced liver injury. Hepatology. 2012; 55:1204–1214. [PubMed: 22105582]
7. Nishina T, Komazawa-Sakon S, Yanaka S, Piao X, Zheng DM, Piao JH, Kojima Y, et al. Interleukin-11 links oxidative stress and compensatory proliferation. Sci Signal. 2012; 5:ra5. [PubMed: 22253262]
8. Sheng L, Zhou Y, Chen Z, Ren D, Cho KW, Jiang L, Shen H, et al. NF-kappaB-inducing kinase (NIK) promotes hyperglycemia and glucose intolerance in obesity by augmenting glucagon action. Nat Med. 2012; 18:943–949. [PubMed: 22581287]
9. Saitoh Y, Yamamoto N, Dewan MZ, Sugimoto H, Martinez Bruyn VJ, Iwasaki Y, Matsubara K, et al. Overexpressed NF-kappaB-inducing kinase contributes to the tumorigenesis of adult T-cell leukemia and Hodgkin Reed-Sternberg cells. Blood. 2008; 111:5118–5129. [PubMed: 18305221]
10. Liao G, Zhang M, Harhaj EW, Sun SC. Regulation of the NF-kappaB-inducing kinase by tumor necrosis factor receptor-associated factor 3-induced degradation. J Biol Chem. 2004; 279:26243–26250. [PubMed: 15084608]
11. Varfolomeev E, Blankenship JW, Wayson SM, Fedorova AV, Kayagaki N, Garg P, Zobel K, et al. IAP antagonists induce autoubiquitination of c-IAPs, NF-kappaB activation, and TNFalpha-dependent apoptosis. Cell. 2007; 131:669–681. [PubMed: 18022362]
12. Vince JE, Wong WW, Khan N, Feltham R, Chau D, Ahmed AU, Benetatos CA, et al. IAP antagonists target cIAP1 to induce TNFalpha-dependent apoptosis. Cell. 2007; 131:682–693. [PubMed: 18022363]
13. Sun SC. Non-canonical NF-kappaB signaling pathway. Cell Res. 2011; 21:71–85. [PubMed: 21173796]

14. Thu YM, Richmond A. NF-kappaB inducing kinase: a key regulator in the immune system and in cancer. Cytokine Growth Factor Rev. 2010; 21:213–226. [PubMed: 20685151]
15. Habib AA, Chatterjee S, Park SK, Ratan RR, Lefebvre S, Vartanian T. The epidermal growth factor receptor engages receptor interacting protein and nuclear factor-kappa B (NF-kappa B)-inducing kinase to activate NF-kappa B. Identification of a novel receptor-tyrosine kinase signalosome. J Biol Chem. 2001; 276:8865–8874. [PubMed: 11116146]
16. Fan S, Meng Q, Laterra JJ, Rosen EM. Role of Src signal transduction pathways in scatter factor-mediated cellular protection. J Biol Chem. 2009; 284:7561–7577. [PubMed: 19047046]
17. Fagarasan S, Shinkura R, Kamata T, Nogaki F, Ikuta K, Tashiro K, Honjo T. Alymphoplasia (aly)-type nuclear factor kappaB-inducing kinase (NIK) causes defects in secondary lymphoid tissue chemokine receptor signaling and homing of peritoneal cells to the gut-associated lymphatic tissue system. J Exp Med. 2000; 191:1477–1486. [PubMed: 10790423]
18. Park GY, Wang X, Hu N, Pedchenko TV, Blackwell TS, Christman JW. NIK is involved in nucleosomal regulation by enhancing histone H3 phosphorylation by IKKalpha. J Biol Chem. 2006; 281:18684–18690. [PubMed: 16675465]
19. Zarnegar BJ, Wang Y, Mahoney DJ, Dempsey PW, Cheung HH, He J, Shiba T, et al. Noncanonical NF-kappaB activation requires coordinated assembly of a regulatory complex of the adaptors cIAP1, cIAP2, TRAF2 and TRAF3 and the kinase NIK. Nat Immunol. 2008; 9:1371–1378. [PubMed: 18997794]
20. Vallabhapurapu S, Matsuzawa A, Zhang W, Tseng PH, Keats JJ, Wang H, Vignali DA, et al. Nonredundant and complementary functions of TRAF2 and TRAF3 in a ubiquitination cascade that activates NIK-dependent alternative NF-kappaB signaling. Nat Immunol. 2008; 9:1364–1370. [PubMed: 18997792]
21. Xiao G, Harhaj EW, Sun SC. NF-kappaB-inducing kinase regulates the processing of NF-kappaB2 p100. Mol Cell. 2001; 7:401–409. [PubMed: 11239468]
22. Senftleben U, Cao Y, Xiao G, Greten FR, Krahn G, Bonizzi G, Chen Y, et al. Activation by IKKalpha of a second, evolutionary conserved, NF-kappa B signaling pathway. Science. 2001; 293:1495–1499. [PubMed: 11520989]
23. Xiao G, Fong A, Sun SC. Induction of p100 processing by NF-kappaB-inducing kinase involves docking IkappaB kinase alpha (IKKalpha) to p100 and IKKalpha-mediated phosphorylation. J Biol Chem. 2004; 279:30099–30105. [PubMed: 15140882]
24. Sasaki Y, Calado DP, Derudder E, Zhang B, Shimizu Y, Mackay F, Nishikawa S, et al. NIK overexpression amplifies, whereas ablation of its TRAF3-binding domain replaces BAFF:BAFF-R-mediated survival signals in B cells. Proc Natl Acad Sci U S A. 2008; 105:10883–10888. [PubMed: 18663224]
25. Usynin IF, Khar'kovsky AV, Balitskaya NI, Panin LE. Gadolinium chloride-induced Kupffer cell blockade increases uptake of oxidized low-density lipoproteins by rat heart and aorta. Biochemistry (Mosc). 1999; 64:620–624. [PubMed: 10395974]
26. Huang W, Metlakunta A, Dedousis N, Zhang P, Sipula I, Dube JJ, Scott DK, et al. Depletion of liver Kupffer cells prevents the development of diet-induced hepatic steatosis and insulin resistance. Diabetes. 2010; 59:347–357. [PubMed: 19934001]
27. Ku NO, Toivola DM, Strnad P, Omary MB. Cytoskeletal keratin glycosylation protects epithelial tissue from injury. Nat Cell Biol. 2010; 12:876–885. [PubMed: 20729838]
28. Shinkura R, Kitada K, Matsuda F, Tashiro K, Ikuta K, Suzuki M, Kogishi K, et al. Alymphoplasia is caused by a point mutation in the mouse gene encoding Nf-kappa b-inducing kinase. Nat Genet. 1999; 22:74–77. [PubMed: 10319865]
29. Sunami Y, Leithauser F, Gul S, Fiedler K, Guldiken N, Espenlaub S, Holzmann KH, et al. Hepatic activation of IKK/NFkappaB signaling induces liver fibrosis via macrophage-mediated chronic inflammation. Hepatology. 2012; 56:1117–1128. [PubMed: 22407857]
30. Jijon H, Allard B, Jobin C. NF-kappaB inducing kinase activates NF-kappaB transcriptional activity independently of IkappaB kinase gamma through a p38 MAPK-dependent RelA phosphorylation pathway. Cell Signal. 2004; 16:1023–1032. [PubMed: 15212763]

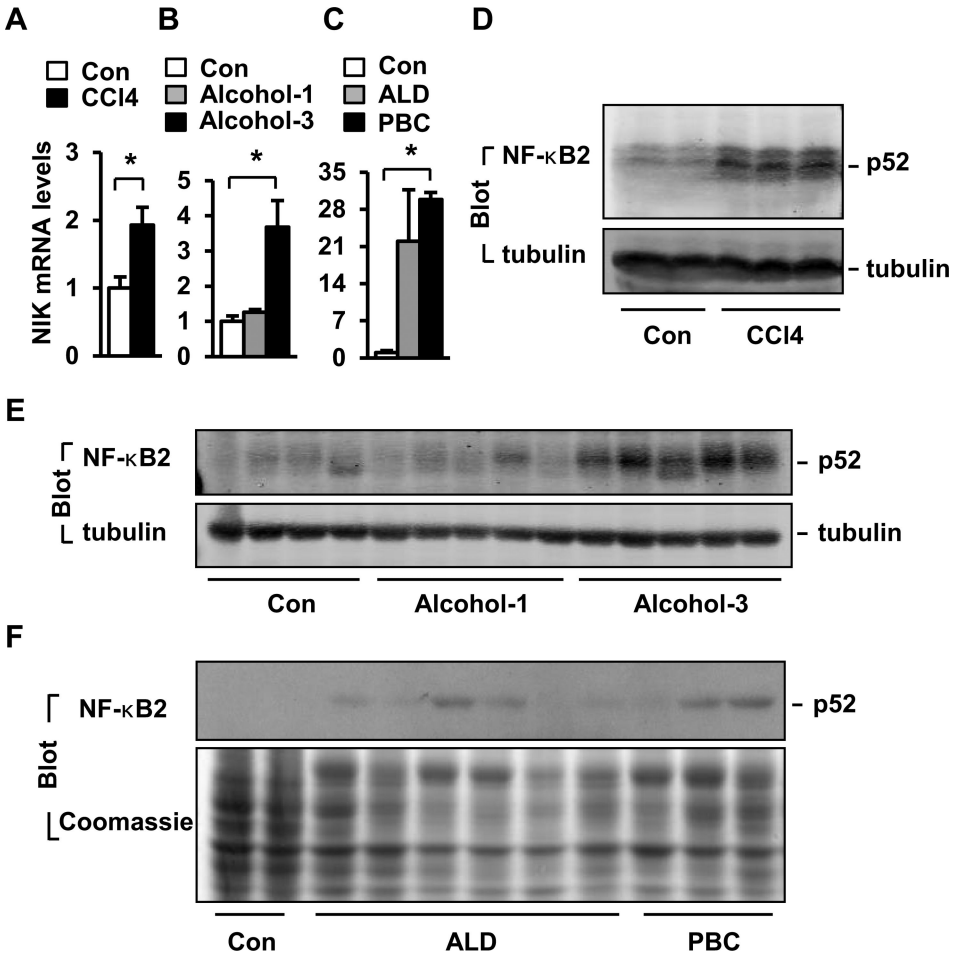

Fig. 1. Liver injury is associated with increased activation of hepatic NIK

(A-B) Liver NIK expression was quantified by qPCR and normalized to 18S levels. Con: n=4, CCl4: n=7; **C**on: n=4, alcohol: n=5. (C) NIK mRNA levels were measured by qPCR in human liver samples and normalized to GAPDH levels. Con: n=2; ALD: n=6; PBC: n=3. (D-E) Liver extracts were immunoblotted with antibodies against NF-κB2 or tubulin. (F) Liver extracts were prepared from human samples and immunoblotted with anti-NF-κB2 antibody. The same blots were stained with Coomassie blue to visualize total proteins. *$p<0.05$.

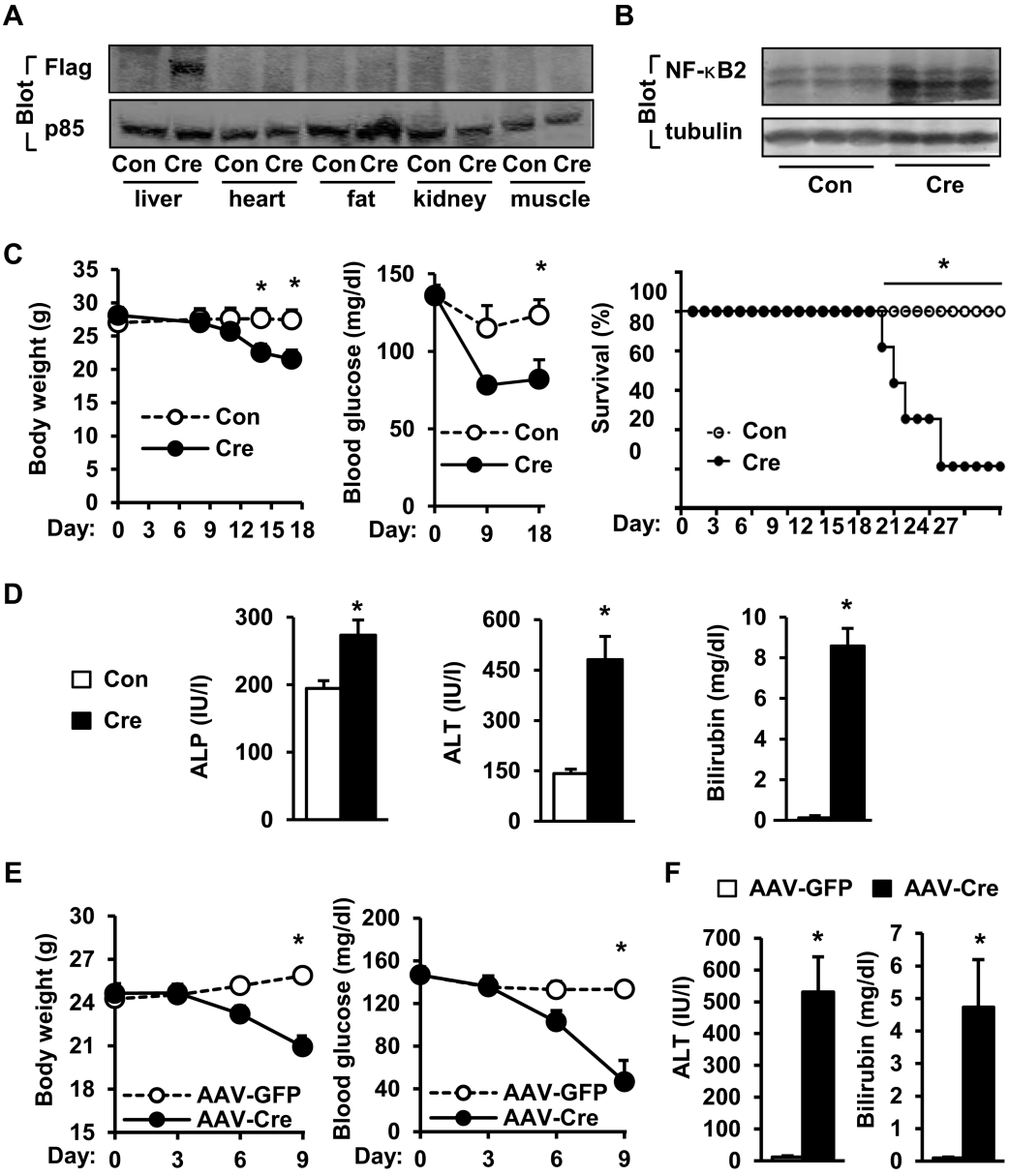

Fig. 2. Adult-onset, hepatocyte-specific overexpression of NIK causes lethal liver injury

(A-B) *STOP-NIK* mice were infected with GFP (Con) or *albumin*-Cre adenoviruses via tail vein injection. Tissue extracts were immunoblotted with the indicated antibodies. (C) Body weight (Con: n=6; Cre: n=6), nonfasting blood glucose (Con: n=4; Cre: n=4), and survival curves (Con: n=4; Cre: n=5). (D) Plasma ALT and ALP activity and total bilirubin levels 18 days after infection. Con: n=6; Cre: n=5. (E) *STOP-NIK* mice were infected with AAV-GFP or AAV-Cre, and body weight and nonfasting blood glucose were monitored. AAV-GFP: n=3; AAV-Cre: n=3. (F) Plasma ALT activity and total bilirubin levels were measured 9 days after infection. AAV-GFP: n=3; AAV-Cre: n=3. *$p<0.05$.

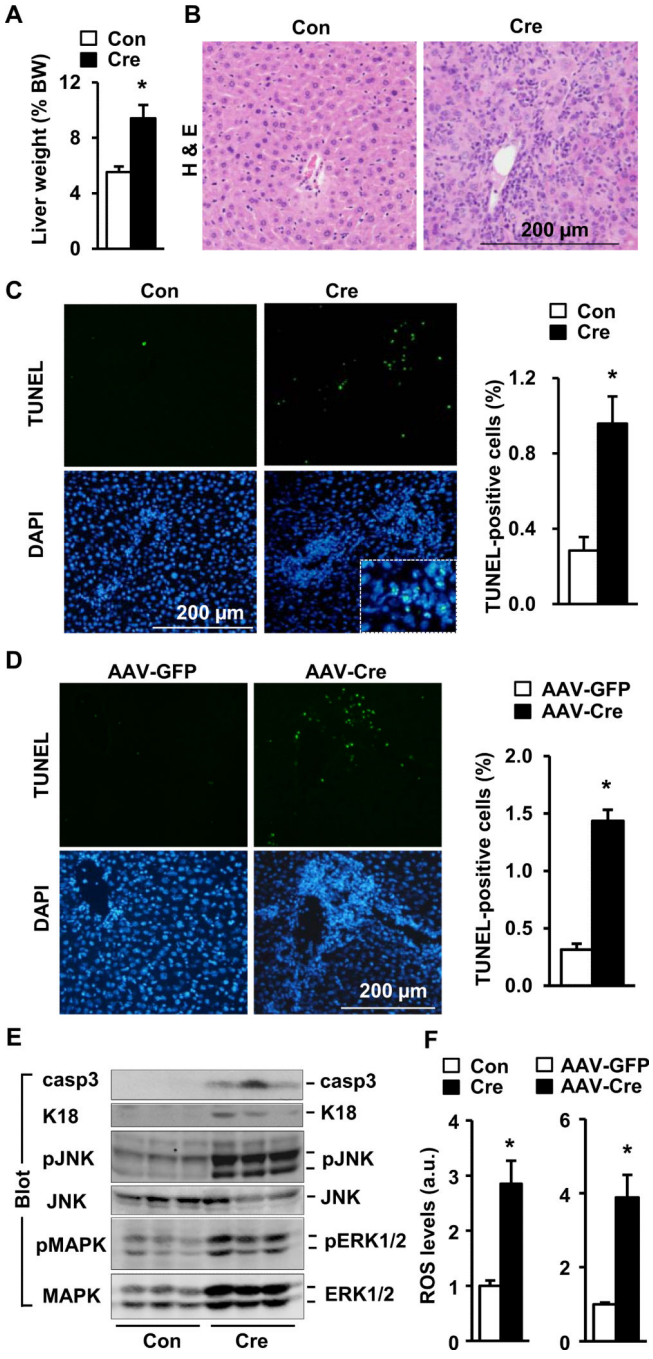

Fig. 3. Adult-onset, hepatocyte-specific overexpression of NIK causes liver oxidative stress and hepatocyte death

(A-C) *STOP-NIK* males were sacrificed 18 days after GFP (Con) or *albumin*-Cre adenoviral infection. (A) Liver weight. BW: body weight. Con: n=6; Cre: n=6. (B) H & E staining of liver sections. (C) Liver sections were co-stained with TUNEL reagents and DAPI. Inserts: enlarged merged images. TUNEL-positive cells were normalized to DAPI-positive cells. Con: n=5; Cre: n=5. (D) *STOP-NIK* mice were infected with AAV-GFP or AAV-Cre, and liver sections (9 days after infection) were stained with TUNEL reagents and DAPI. AAV-

GFP: n=3; AAV-Cre: n=3. (E) Liver extracts (18 days after adenoviral infection) were immunoblotted with the indicated antibodies. (F) Liver ROS levels (normalized to protein levels). a.u.: arbitrary units. Con: n=6; Cre: n=5; AAV-GFP: n=3; AAV-Cre: n=3. *$p<0.05$.

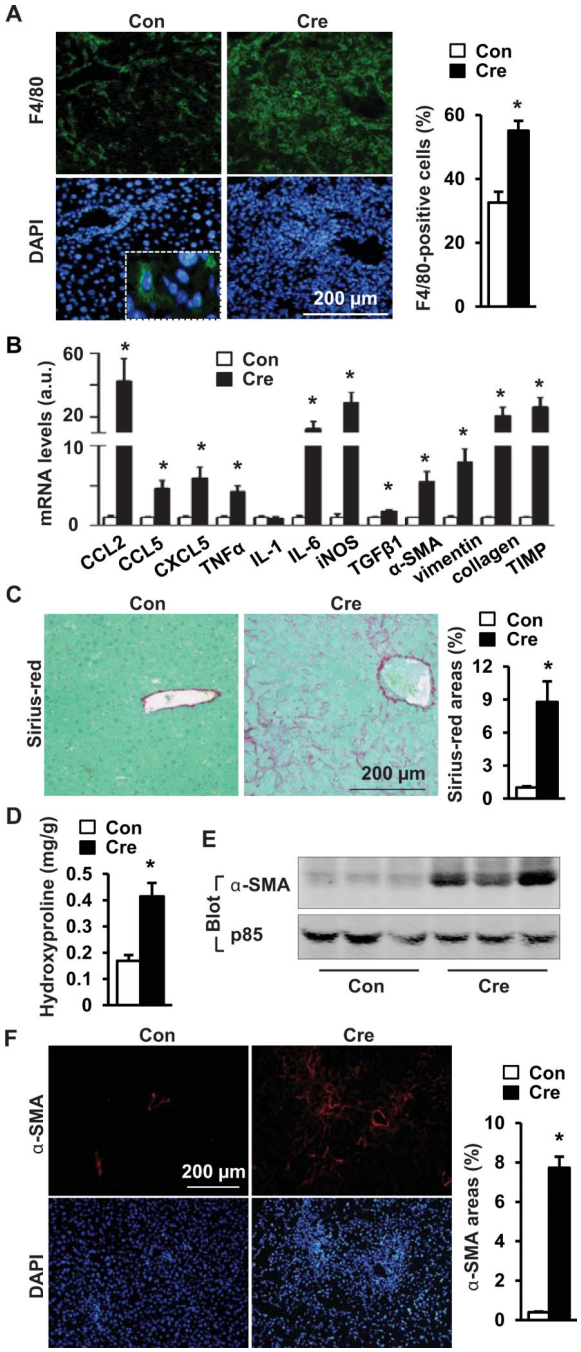

Fig. 4. Adult-onset, hepatocyte-specific overexpression of NIK causes liver inflammation and fibrosis

STOP-NIK males were sacrificed 18 days after GFP (Con) or *albumin*-Cre adenoviral infection. (A) Liver sections were immunostained with anti-F4/80 antibody. F4/80-positive cells were normalized to DAPI-positive cells. Con: n=6; Cre: n=5. (B) The abundance of hepatic mRNAs (normalized to 18S levels). Con: n=5-6; Cre: n=6. (C) Liver sections were stained with Sirius-red/fast green. Sirius-red-positive areas were normalized to total microscopic areas. Con: n=6; Cre; n=6. (D) Liver hydroxyproline levels (normalized to liver weight). Con: n=6; Cre, n=6. (E) Liver extracts were immunoblotted with antibodies against

α-SMA or p85. (F) Liver sections were immunostained with antibody to α-SMA. α-SMA-positive areas were normalized to microscopic areas. Con: n=4; Cre: n=4. *$p<0.05$.

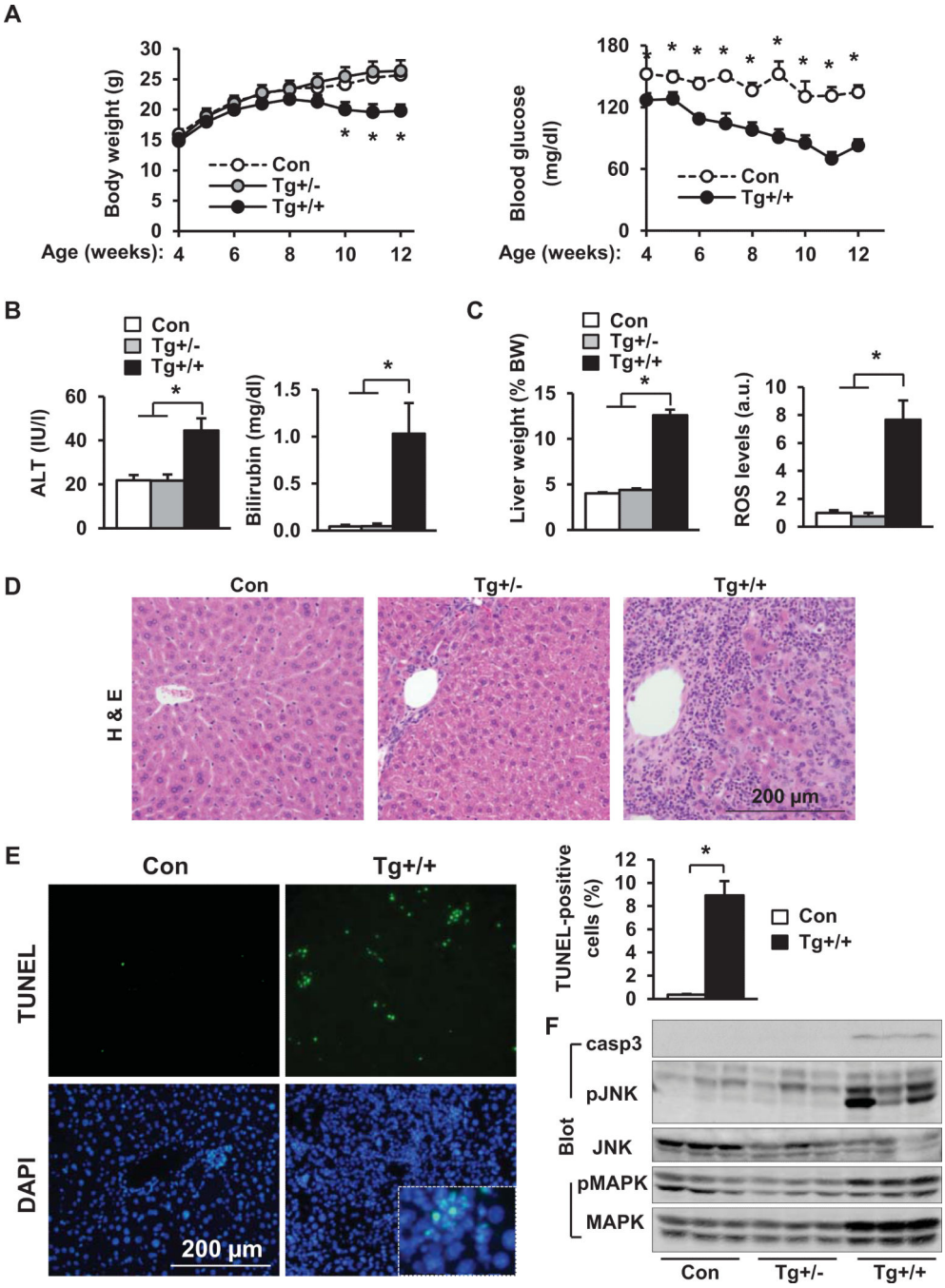

Fig. 5. Embryonic onset, hepatocyte-specific overexpression of NIK causes liver oxidative stress, hepatocyte death, and liver injury

(A) Body weight and blood glucose levels. *: Con vs $Tg^{+/+}$. Con: n=5-7; $Tg^{+/-}$: n=5; $Tg^{+/+}$: n=7-9. (B) Blood ALT and total bilirubin levels at 13 weeks of age. Con: n=7; $Tg^{+/-}$: n=3-5; $Tg^{+/+}$: n=9. (C-F) Mice were sacrificed at 13 weeks of age. (C) Liver weight and ROS levels (normalized to total protein levels). Con: n=7; $Tg^{+/-}$: n=3; $Tg^{+/+}$: n=8-9. (D) H & E staining of liver sections. (E) TUNEL-positive cells (normalized to DAPI-positive cells). Con: n=5; $Tg^{+/+}$: n=5. (F) Liver extracts were immunoblotted with the indicated antibodies. *$p<0.05$.

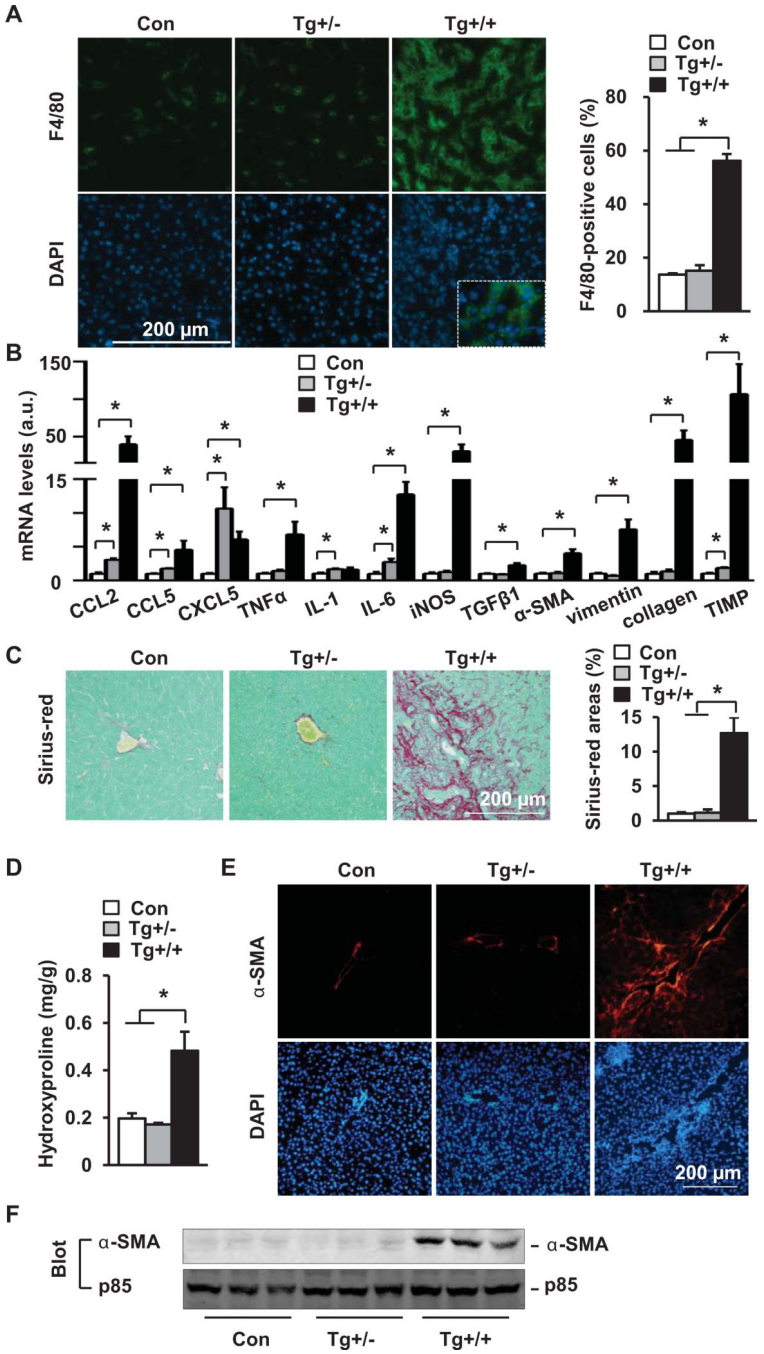

Fig. 6. Embryonic onset, hepatocyte-specific overexpression of NIK causes liver inflammation and fibrosis

(A) Liver sections were immunostained with anti-F4/80 antibody (normalized to DAPI-positive cells). Con: n=5; $Tg^{+/-}$: n=3; $Tg^{+/+}$: n=5. (B) Liver mRNA abundance. Con: n=4-5; $Tg^{+/-}$: n=3; $Tg^{+/+}$: n=5. (C) Liver sections were stained with Sirius-red/fast green. Con: n=5; $Tg^{+/-}$: n=3; $Tg^{+/+}$: n=6. (D) Liver hydroxyproline levels. Con: n=7; $Tg^{+/-}$: n=3; $Tg^{+/+}$: n=8. (E) Liver sections were immunostained with antibody to α-SMA. (F) Liver extracts were immunoblotted with antibodies against α-SMA or p85. *$p<0.05$.

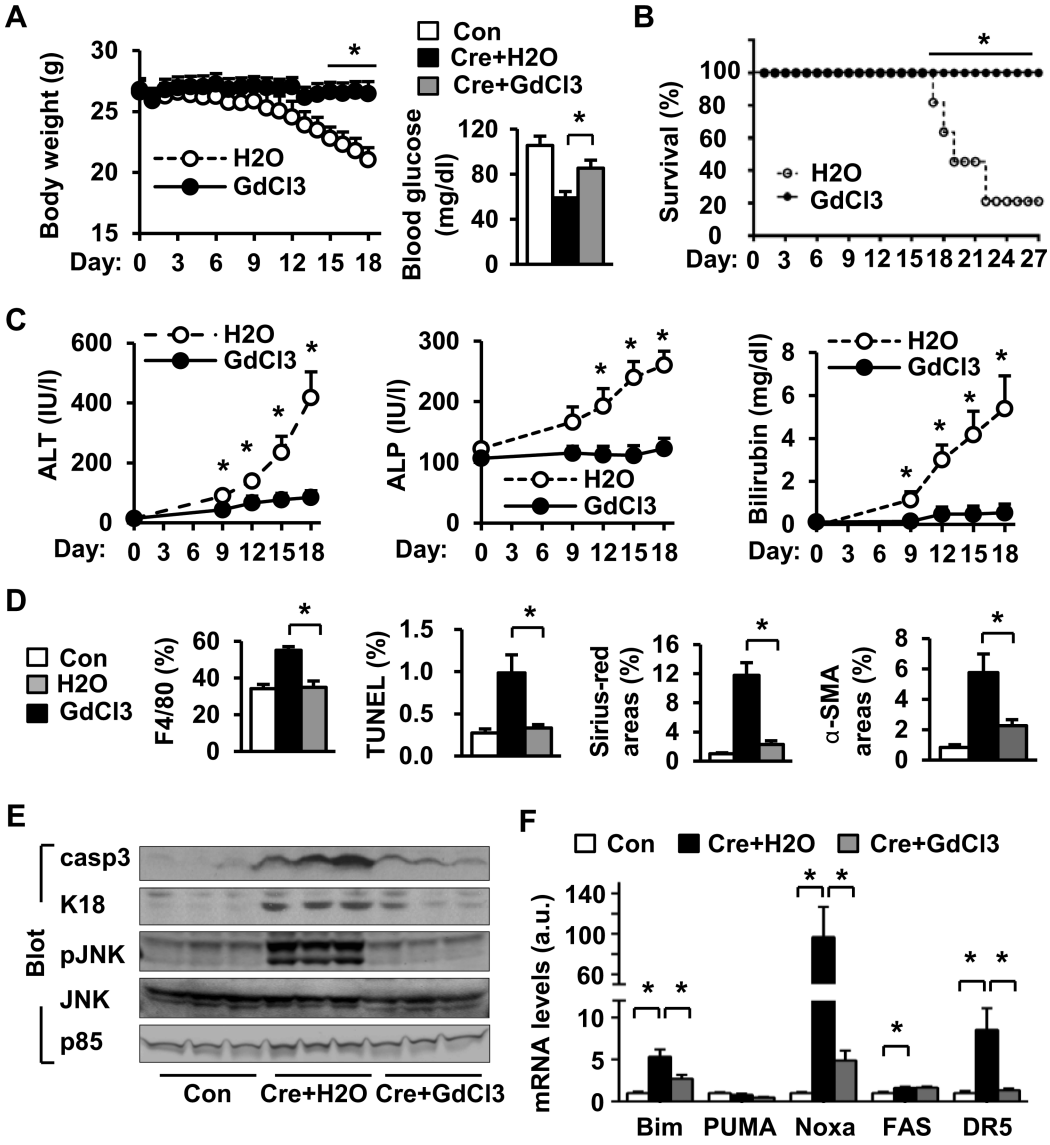

Fig. 7. Depletion of Kupffer cells/macrophages attenuates NIK's detrimental effects

(A) Body weight (H_2O: n=6; $GdCl_3$: n=6) and fasting (5 h) blood glucose levels (18 days after *albumin*-Cre infection, Con: n=6; Cre+H_2O: n=12; Cre+$GdCl_3$: n=6). (B) Survival rates. H_2O: n=5; $GdCl_3$: n=5. (C) Plasma ALT and ALP activity and total bilirubin levels 18 days after *albumin*-Cre infection. H_2O: n=6-8; $GdCl_3$: n=6. (D) Liver sections were stained with TUNEL, Sirius-red/fast green, or antibodies to F4/80 or α-SMA. Con: n=4-6; Cre +H_2O: n=4-7; Cre+$GdCl_3$: n=5-6. (E) Liver extracts were immunoblotted with the indicated antibodies. (F) The mRNA levels in the liver (normalized to 18S levels). Con: n=6; Cre +H_2O: n=6; Cre+$GdCl_3$: n=5. *$p<0.05$.

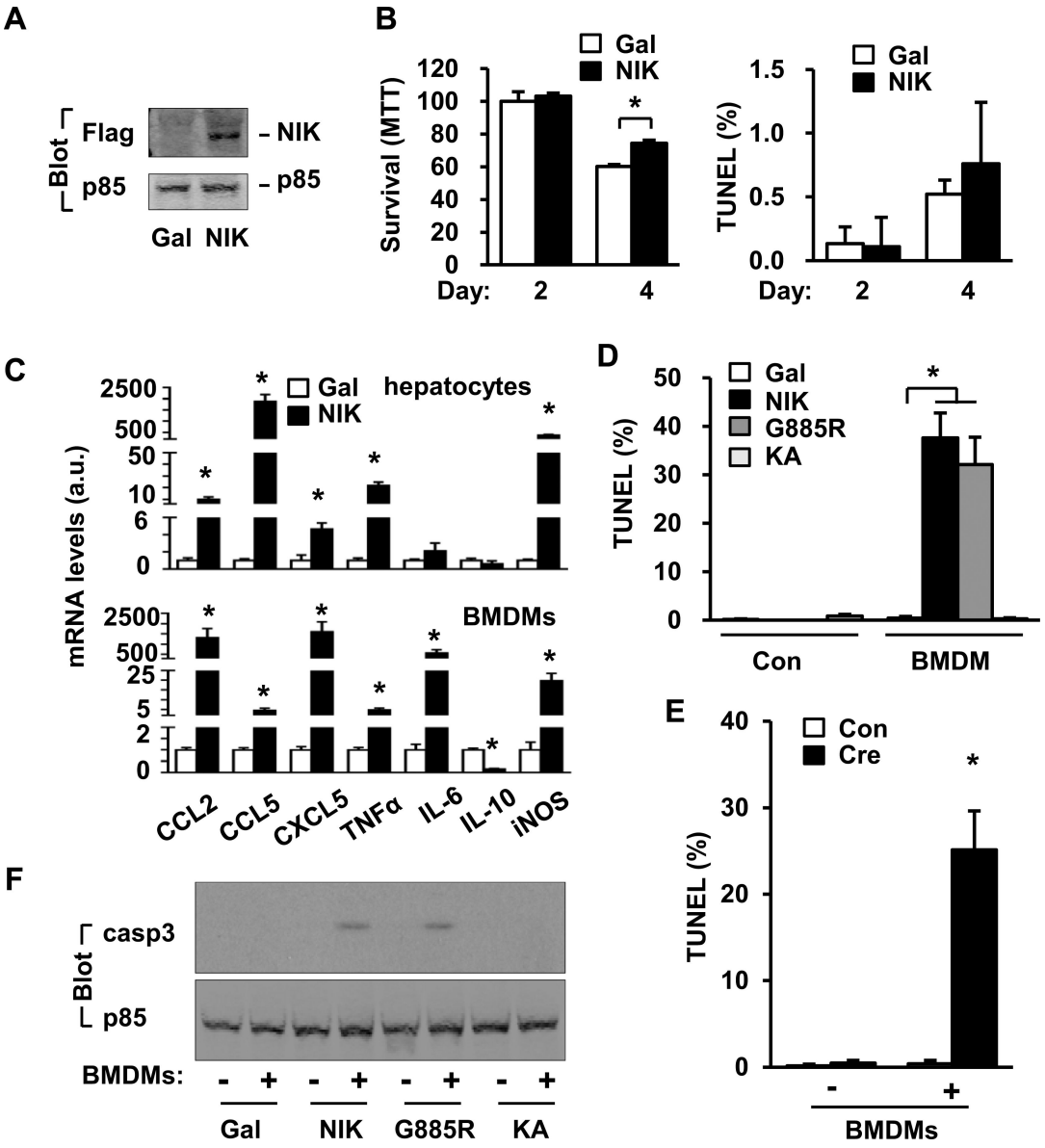

Fig. 8. Hepatic NIK triggers BMDM-dependent hepatocyte apoptosis

(A) Primary hepatocytes were infected with β-Gal or NIK adenoviruses. Cell extracts were immunoblotted with the indicated antibodies. (B) Cell survival and apoptosis. MTT: Gal: n=3, NIK: n=3; TUNEL: Gal: n=5; NIK: n=5. (C) Primary hepatocytes were infected with β-Gal (n=3) or NIK (n=3) adenoviruses. Gene expression was measured by qPCR 42 h after infection. BMDMs were treated with NIK (n=3) or β-Gal (n=3) conditioned medium. Gene expression was measured 18 h after treatments. (D) Primary hepatocytes were infected with β-Gal, NIK, G885R or KA adenoviruses and co-cultured with BMDMs for 2 days. Hepatocytes were stained with TUNEL reagents, and TUNEL-positive cells were normalized to DAPI-positive cells. Gal: n=5; NIK: n=5; G855R: n=5; KA: n=5. (E) Primary hepatocytes were isolated from *STOP-NIK* mice and infected with GFP (Con, n=5) or *albumin*-Cre (n=5) adenoviruses, and TUNEL assays were performed in the absence or presence of BMDMs (3 days). (F) Primary hepatocytes were infected with the indicated

adenoviruses and co-cultured with or without BMDMs for 2 days. Cell lysates were immunoblotted with the indicated antibodies. *$p<0.05$.